TSUNAMI INUNDATION MODELING FOR COASTAL ZONE OF ALEXANDRIA CITY

Mohamed Elsayed[*] **Supervisor: Yushiro FUJII**[**]
MEE17720 **Bunichiro SHIBAZAKI**[**]

ABSTRACT

The Alexandria's coastal zone suffered from disastrous tsunamigenic earthquakes; the 142, 365, 1303, and 1222 earthquakes that were mainly produced from the Hellenic and Cyprian arcs. We focused on the Alexandria middle coastal zone to investigate tsunami propagation and inundation by adopting the assumed fault models for the earthquakes. Using TUNAMI (Tohoku University's Numerical Analysis Model for Investigation) code, we performed numerical simulations and constructed inundation maps. We downloaded bathymetry data of GEBCO 30 arc-sec and topographic data of SRTM 1 arc-sec. We divided the computation domain into four grids, such as the finest grid represented inundated area merging GEBCO and SRTM data. We set six coastal output points along the Egyptian shoreline including the real Alexandria gauge to study tsunami height and arrival time. Moreover, we picked out five important points to evaluate tsunami run-up height and inundated depth. Our computation results showed that the first wave arrived at the coastline of the Alexandria after 62 min of the 142 earthquake with the maximum tsunami run-up height of 6.48 m and inundated depth of 7.63 m. While, the 1222 source closest to Alexandria had the maximum tsunami run-up height of 0.55 m and inundated depth of 1.2 m. Computed inundation maps showed that the 142 event covered the largest inundation area than other events. For all sources, the western inundated areas were much wider than the eastern inundated areas.

Keywords: Alexandria, Tsunami Propagation, Tsunami Heights, Run-Up Heights, Inundation Depth.

1. INTRODUCTION

Recently, after the occurrence of two local tsunamis in the Eastern Mediterranean Sea (EMS): the one in Algeria in 2003 (Mw = 6.8) and the other one in Turkey in 2017 (Mw = 6.6). These events verified the capability of EMS to generate the tsunami in the future. Also, understanding the effect of tsunami propagation and inundation is extremely important for the disaster preparedness in the planning and protection of coastal areas. Alexandria city is located at the center of northern Egyptian shoreline along the EMS. It is the oldest and the second largest city in Egypt regarding the population as well as a major industrial and economic centers. Historically, Alexandria was exposed to a few disastrous events: the 365, 142, 1303 earthquakes along the Hellenic arc and 1222 earthquake along the Cyprian arc (Figure 1) (Fokaefs and Papadopoulos, 2007; Valle et al., 2014). Nevertheless, there are no near-field faults reported seriously to generate a tsunami in Alexandria. Such events do not comprise run-up height or inundation extension on land. Therefore, we must pay attention to this region for increasing the awareness of hazardous events and inundation.

[*]National Research Institute of Astronomy and Geophysics (NRIAG), Seismology department, Egyptian National Seismic Network (ENSN), Egypt.
[**]International Institute of Seismology and Earthquake Engineering, Building Research Institute, Japan.

2. DATA USED FOR TSUNAMI MODELING

2.1. Bathymetry and topography data

For tsunami simulation and inundation modelings, we downloaded bathymetry data of 30 arc-sec grid in EMS from the General Bathymetric Chart of the Ocean (GEBCO) 2014 (Wetherall et al., 2015) (http://www.gebco.net/). As topography data is crucial to perform tsunami inundation modeling, we also downloaded data of 1 arc-sec grid from Shutter Radar Topographic Mission (SRTM) website (https://earthexplorer.usgs.gov/) to obtain accurate results.

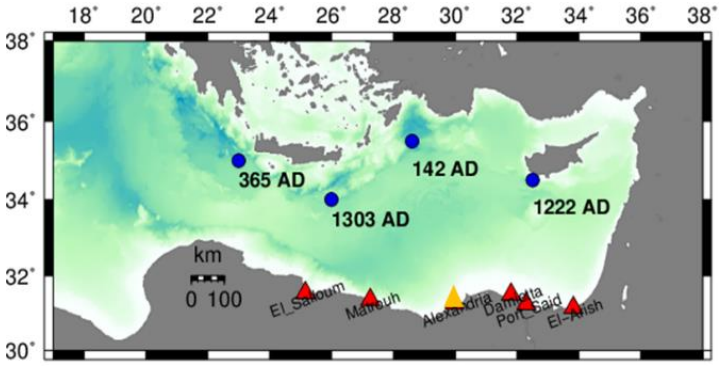

Figure 1. Location of historical tsunamigenic earthquakes (blue circles). Six coastal output points are also shown by yellow triangle (existing tide gauge in Alexandria) and red triangles (virtual tide gauges).

2.2. Computational regions and settings

We divided the computation area into four regions that are Regions 1, 2, 3, and 4 to study tsunami inundation. Region 1 covers EMS as the whole region of the computation domain with the coarsest grid. For the inundation area, Region 4 covers smaller area with the finest grid constructed from GEBCO and SRTM data (Figure 2). Table 1 lists the computation parameters for each region with spatial resolutions of data.

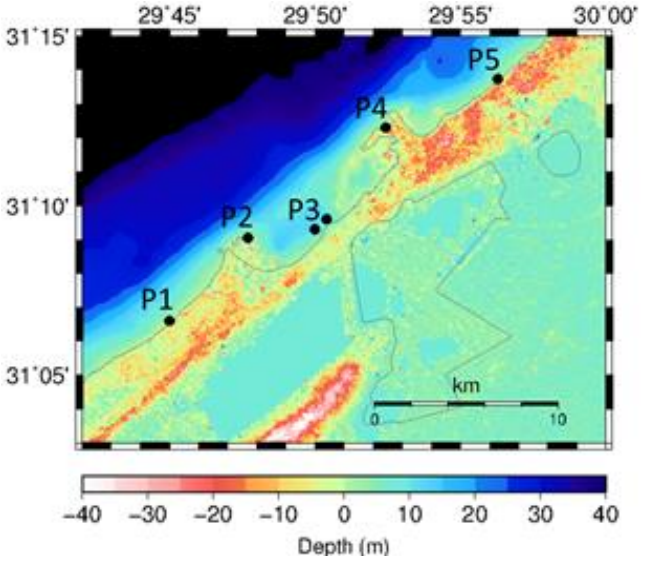

Figure 2. Merged bathymetry and topography data with location of coastal output points (P1 – P5) in Region 4.

Table 1. Computational dimensions and data used for tsunami simulation.

Region	Longitude(°E)	Latitude (°N)	Bathymetry & Topography data	Grid Size dx (m) × dy (m)	Grid Dimension nx × ny
Region 1	18 - 36.5	30 - 37.5	GEBCO 30 arc - sec	1 arc-min 1540 × 1848	1110 × 450
Region 2	28.5- 31.5	30.75 -32		20 arc-sec 514 × 616	540 × 225
Region 3	29.5 - 30.5	30.91 - 31.66		6.66667 arc-sec 171 × 205	540 × 405
Region 4	29.7- 30	31.05 - 31.25	GEBCO 30 arc-sec +SRTM 1 arc - sec	2.22222 arc-sec 57 × 68	486 × 324

2.3. Fault parameters of tsunami sources

We adopted the fault models that were assumed by Valle et al. (2014) for the 142 earthquake and Hamouda (2010) for the 1222 earthquake (Table 2) in order to achieve the main purpose of studying tsunami propagation and inundation.

Table 2. Fault parameters for the 142 and 1222 earthquakes.

Year	Source	Mw	Fault location		Length	Width	Strike	Dip	Rake	Slip	Top depth
			Lon (°E)	lat (°N)	km	km	deg	deg	deg	m	km
142	Valle et al. (2014)	8.6	28.6	35.5	190	90	235	20	90	10	7.5
1222	Hamouda (2010)	7.8	32.5	34.5	80	30	305	35	110	3	15

3. THEORETICAL CONCEPTS AND METHODOLOGY

To simulate the tsunami propagation and inundation, we applied the theory of nonlinear shallow water in the spherical coordinate system based on the following governing equations namely, continuity Eq. (1) and momentum Eqs. (2) and (3) (Yanagisawa, 2018).

$$\frac{\partial \eta}{\partial t} + \frac{1}{Rcos\theta}\left[\frac{\partial M}{\partial \lambda} + \frac{\partial}{\partial \theta}(Ncos\theta)\right] = 0 \tag{1}$$

$$\frac{\partial M}{\partial t} + \frac{gD}{Rcos\theta}\frac{\partial \eta}{\partial \lambda} + \frac{1}{Rcos\theta}\frac{\partial}{\partial \lambda}\left(\frac{M^2}{D}\right) + \frac{1}{Rcos\theta}\frac{\partial}{\partial \theta}\left(cos\theta\frac{MN}{D}\right) + \frac{\tau_{bx}}{P} = 0 \tag{2}$$

$$\frac{\partial N}{\partial t} + \frac{gD}{Rcos\theta}\frac{\partial}{\partial \theta}(cos\theta\eta) + \frac{1}{Rcos\theta}\frac{\partial}{\partial \lambda}\left(cos\theta\frac{N^2}{D}\right) + \frac{1}{Rcos\theta}\frac{\partial}{\partial \lambda}\left(\frac{MN}{D}\right) + \frac{\tau_{by}}{P} = 0 \tag{3}$$

where λ and θ are the latitude and longitude, η is the elevation of water surface, D is total water depth of $\eta + h$ (still water depth), and R is the earth radius. M and N are the component of discharge along θ and λ. $\frac{\tau_{bx}}{P} = \frac{gn^2}{D^{\frac{7}{3}}}M\sqrt{M^2+N^2}$ and $\frac{\tau_{by}}{P} = \frac{gn^2}{D^{\frac{7}{3}}}N\sqrt{M^2+N^2}$ are the bottom frictional terms.

3.1. Tsunami numerical stability

We can eschew unexpected instability errors by allocating the suitable time step to satisfying the Courant Fredric Lewy (CFL) stability conditions (Imamura et al., 2006), which is determined by $\Delta t \leq \Delta x/\sqrt{2gh_{max}}$

where Δt and Δx are temporal and spatial grid size, g is gravity acceleration (9.8 ms^{-2}) and h_{max} is still maximum water depth in the computation domain. We set the temporal time step (Δt) to be 1 sec. The total calculation time for tsunami propagation is 21,600 sec. Table 3 shows the Δt values for each region in the computation domain.

Table 3. Temporal grid size for tsunami simulation.

Region	1	2	3	4
Δt (sec)	1.00	1.00	1.00	1.00
Δx (m)	1540	513.3	171.1	57.0
$h_{max}(m)$	5128	2644	1218	82.7
$\frac{\Delta x}{\sqrt{2gh_{max}}}$	4.85	2.25	1.10	1.4

4. RESULTS AND DISCUSSION

4.1. Seafloor deformation

The initial step for the tsunami generation and propagation is to calculate the sea bottom displacement using the elastic theory (Okada, 1985). Figure 3 shows the seafloor displacement for the 142 Mw 8.6 and the 1222 Mw 7.8 earthquakes. For the 142 event, the uplift and subsidence are 4.73 m and 1.38 m, but for the 1222 event they are 0.99 m and 0.13 m.

4.2. Tsunami propagation

Figure 4 shows snapshots of tsunami propagation at 0, 60, 90 min for the 142 and 1222 earthquakes to study the tsunami wave behaviors. For the 142 earthquake, the first wave reached to the Alexandria's coastal zone with positive amplitude. We selected five points P1 to P5 as shown in Figure 2 to study tsunami waveforms in Region 4 including the real existing Alexandria tide gauge (next to P3) as coastal point in Region 1. The time history of the calculated tsunami waveforms at the six coastal output points are shown in Figure 5. For the case of the 1222 earthquake, the first wave has also positive amplitude, which it is the closest event to Alexandria.

4.3. Tsunami height and tsunami travel time

Figure 6 shows the computed Maximum Tsunami Height (MTH) at Alexandria. For the 142 event, the MTH was 5.41 m after 62 min (60-65 min). It could be risky at Alexandria city, especially for the western side as it is characterized by lowlands and possesses more upgrading coastal buildings. For the 1222 event, the MTH did not exceed 1 meter (0.55 m) after 73 min (70-75 min). Figure 7 shows the tsunami arrival time at the six output points.

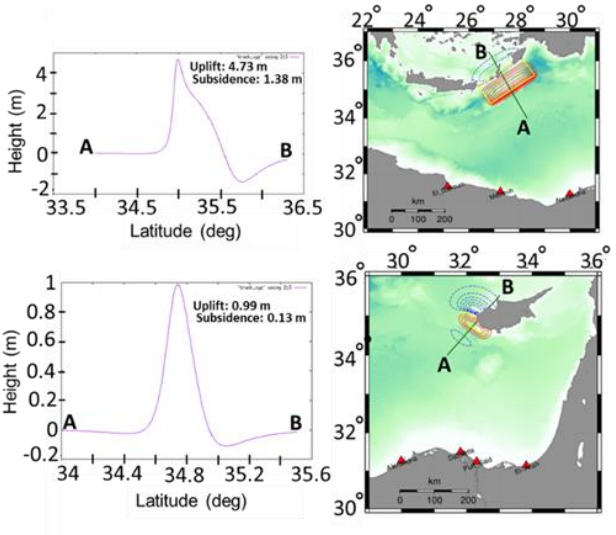

Figure 3. Seafloor displacement computed for the 142 (top) and 1222 (bottom) events. The red and blue colors are uplift and subsidence (right). Red and blue contour lines interval of the 142 are 0.5 m, but for the 1222 they are 0.2 m and 0.02 m. Vertical displacement is shown along cross section AB (left).

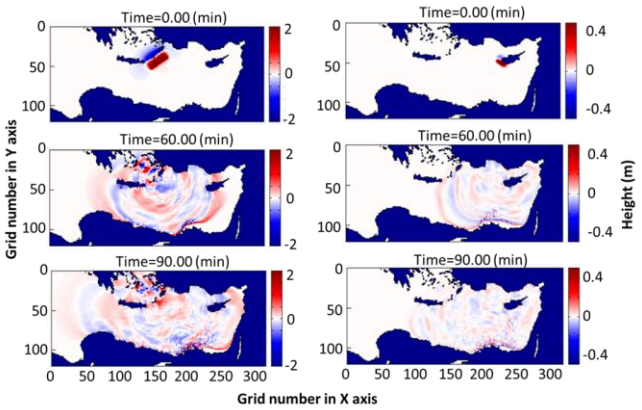

Figure 4. Snapshots of tsunami propagation for the 142 (left) and 1222 (right) earthquakes.

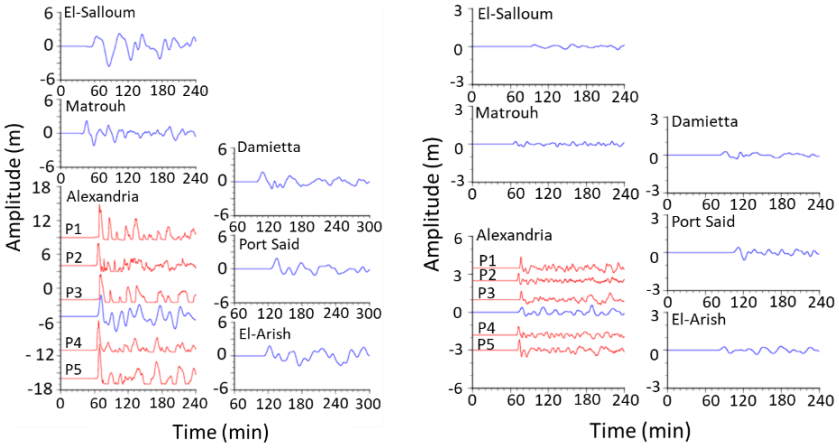

Figure 5. Output tsunami waveforms in Region 1 (blue colors) and five points in Region 4 (red colors) for the 142 (left) and 1222 (right) events.

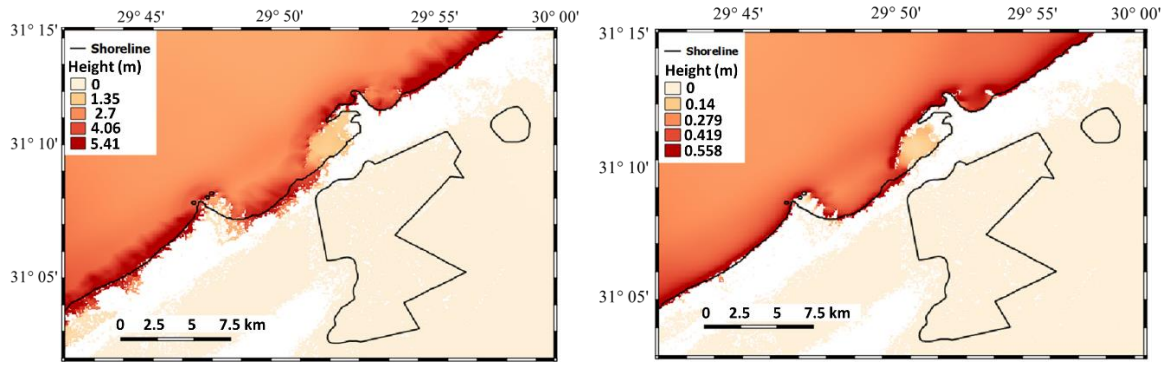

Figure 6. Tsunami height for the 142 (left) and 1222 (right) earthquakes.

4.4. Tsunami run-up height

Figure 8 shows the location of five significant points that were selected nearly the coastline while Figure 9 represents the tsunami evaluated run-up heights. The maximum computed tsunami run-up height of 6.4 m was recorded at Bibliotheca Alexandrina as it is topographically more elevated than other selected points. These values were gradually increased in the eastern coastline except for Alexandria port as it is protected by seawall and the Citadel of Qaitbay as it is mainly constructed so near to the shoreline.

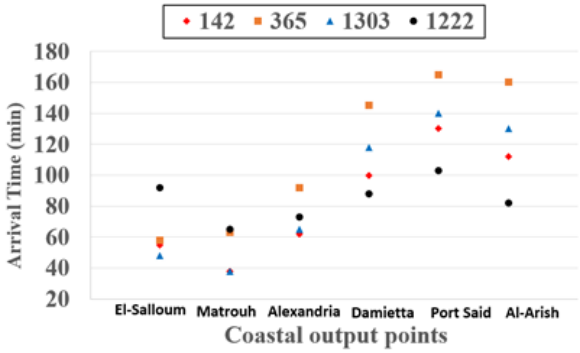

Figure 7. Tsunami arrival time.

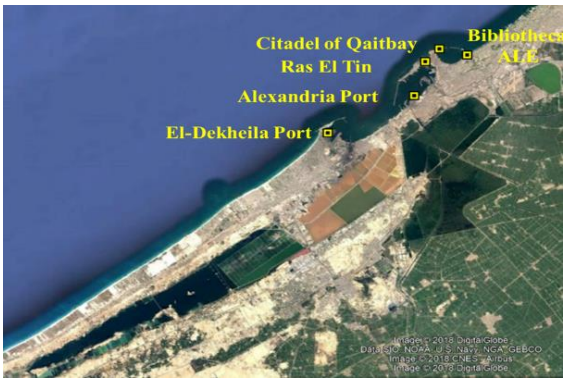

Figure 8. Location of evaluation points (Source: google earth).

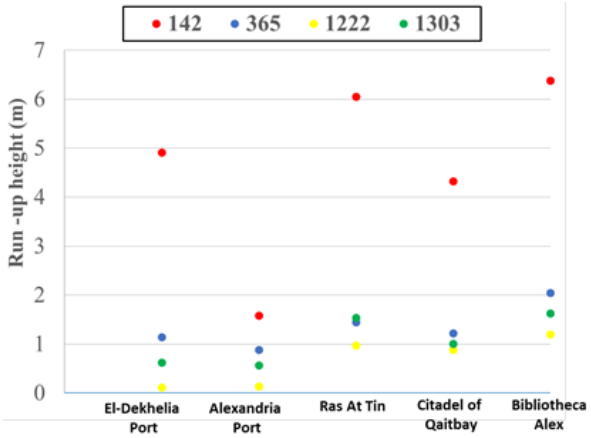

Figure 9. Evaluated tsunami run-up heights.

4.5. Tsunami inundation

The case of the 142 earthquake covered larger inundated areas than other events due to probably the longest length of tsunami source, the shallow top depth of the fault and the directivity of tsunami wave energy towards Alexandria (Figure 10). The maximum elevation of water on land for this event is estimated to be 7.63 m. Conversely, the shape of the inundated area for the 1222 earthquake represented the smallest and limited inundated areas with the calculated maximum inundation depth of 1.2 m (Figure 11).

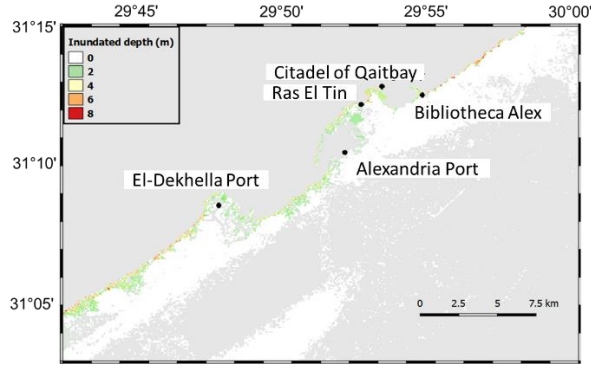

Figure 10. Inundated water depth for the 142 event.

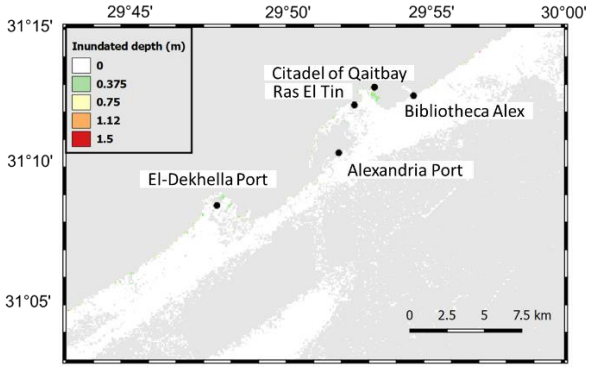

Figure 11. Same as Figure 10, but for the 1222 event.

5. CONCLUSIONS

Using TUNAMI code, tsunami simulation and inundation results show that the maximum run-up height and inundated depth were 6.48 m and 7.63 m for the 142 event with inundated horizontal distance of about 1,550 m from a coastline. While, the 1222 event as the less risky source had the maximum tsunami height and run-up height of less than 1 m. It would be hazardous particularly for people swimming or standing on a beach with the inundation distance of about 650 m. For all earthquake sources, the maximum run-up height was recorded at Bibliotheca Alexandrina as its highly elevated, whilst the Alexandria port represented the least computed run-up height and inundated depth as it is protected by the breakwater. The Ras el Tin area was highly inundated. Western coastline areas were more exposed and vulnerable to inundation than the eastern coastline as it is topographically more lowland areas.

6. RECOMMENDATIONS

1. A precise local bathymetry and topography data are required for accurate results in tsunami modeling.
2. Preserving of barriers, large boulders and some ponds and channels are considered as one of the initial steps for disaster preparedness and mitigations in future tsunami risk in Alexandria.
3. Besides, early warning systems and evacuation planning are a key to minimize tsunami casualties and economic losses.

ACKNOWLEDGEMENTS

I would like to express my sincere gratitude to my supervisor Dr. FUJII and my supervisor and advisor Dr. SHIBAZAKI for their continuous support, valuable guidance and suggestions during my study.

REFERENCES

Fokaefs, A., and Papadopoulos, G.A., 2007, Natural Hazards 40.3, 503-526.
Hamouda, A.Z., 2010, Marine Geophysical Researches, 31.3, 197-214.
Imamura, F., Yalciner, A.C., and Ozyurt, G., 2006, DCRC, Tohoku University, Japan.
Okada, Y., 1985, Bulletin of the Seismological Society of America, 75(4), 1135-1154.
Valle, B. L., et al., 2014, Proceedings of the Institution of Civil Engineers-Engineering and Computational Mechanics, 167(3), 99-105.
Weatherall, P., et al., 2015, Earth and Space Science, 2, 331–345.
Yanagisawa, H., 2018, IISEE, BRI, Japan.